A Unified Model for the Analysis of FACTS Devices in Damping Power System Oscillations—Part III: Unified Power Flow Controller

HaiFeng Wang, *Member, IEEE*

***Abstract*—This paper presents the establishment of the linearized Phillips–Heffron model of a power system installed with a Unified Power Flow Controller (UPFC). Two applications based on the Phillips–Heffron model are demonstrated: 1) Study on the effect of UPFC DC voltage regulator on power system oscillation stability; 2) Selection of damping control signal for the design of UPFC damping controller.**

***Index Terms*—FACTS, Phillips–Heffron model, power system dynamic stability, power system modeling, UPFC.**

I. Introduction

THE UNIFIED Power Flow Controller (UPFC) was proposed [1] for the Flexible AC Transmission Systems (FACTS), which is a multiple-functional FACTS controller with primary duty to be power flow control. The secondary functions of the UPFC can be voltage control, transient stability improvement, oscillation damping [2]–[4], etc. In [2] and [3], it is demonstrated by examples that the UPFC can be very effective to damp power system oscillations. So far, however, the damping function of the UPFC has not been investigated thoroughly. In this paper, the linearized Phillips–Heffron model [8], [9] of a power system installed with a UPFC is derived which turns out to be of the exactly same form as that of the unified model presented in [10] and [11] for SVC, TCSC and TCPAR. Thus methods proposed in [10] and [11] based on the Phillips–Heffron model can be directly applied for the analysis and design of UPFC damping control function, which is not to be repeated in the paper. Instead, two applications based on the Phillips–Heffron model which are special to UPFC are demonstrated: 1) Study on the effect of UPFC DC voltage regulator on power system oscillation stability; 2) Selection of damping control signal for the design of UPFC damping controller.

II. Single-Machine Infinite-Bus Power Systems

Fig. 1 is a single-machine infinite-bus power system installed with a UPFC which consists of an excitation transformer (ET), a boosting transformer (BT), two three-phase GTO based voltage source converters (VSC's) and a DC link capacitor. In Fig. 1, m_E, m_B, δ_E and δ_B are the amplitude modulation ratio and phase angle of the control signal of each VSC respectively, which are the input control signals to the UPFC.

Manuscript received November 3, 1998; revised January 26, 2000.
The author is with the University of Bath, Bath, UK.
Publisher Item Identifier S 0885-8977(00)08132-2.

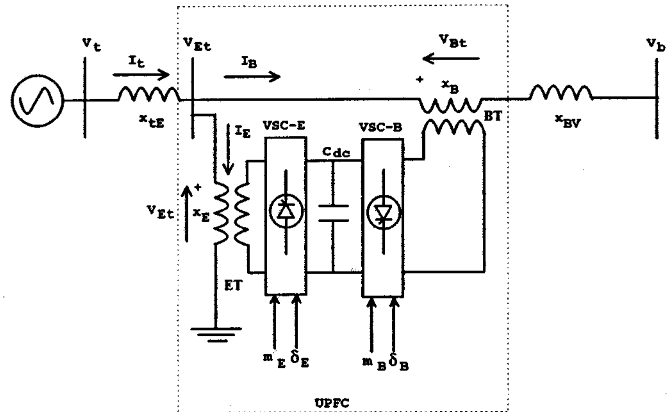

Fig. 1. A UPFC installed in a single-machine infinite-bus power system.

By applying Park's transformation on the three-phase dynamic differential equations of the UPFC and ignoring the resistance and transients of the transformers, the dynamic model of the UPFC is [3]

$$\overline{V}_E = \frac{m_E v_{dc}}{2} e^{j\delta_E}, \quad \overline{V}_B = \frac{m_B v_{dc}}{2} e^{j\delta_B} \tag{2.1}$$

$$\frac{dv_{dc}}{dt} = \frac{3m_E}{4C_{dc}} [\cos\delta_E \quad \sin\delta_E] \begin{bmatrix} i_{Ed} \\ i_{Eq} \end{bmatrix} + \frac{3m_B}{4C_{dc}} [\cos\delta_B \quad \sin\delta_B] \begin{bmatrix} i_{Bd} \\ i_{Bq} \end{bmatrix} \tag{2.2}$$

From Fig. 1 we can have

$$\overline{V}_t = jx_{tE}\overline{I}_t + \overline{V}_{Et}$$
$$\overline{V}_{Et} = \overline{V}_{Bt} + jx_{BV}\overline{I}_B + \overline{V}_b$$

from which we can obtain

$$i_{Ed} = \frac{x_{BB}}{x_{d\Sigma}} E_q' - \frac{m_E \sin\delta_E v_{dc} x_{Bd}}{2x_{d\Sigma}} + \frac{x_{dE}}{x_{d\Sigma}} \left(V_b \cos\delta + \frac{m_B \sin\delta_B v_{dc}}{2} \right)$$

$$i_{Eq} = \frac{m_E \cos\delta_E v_{dc} x_{Bq}}{2x_{q\Sigma}} - \frac{x_{qE}}{x_{q\Sigma}} \left(\frac{m_B \cos\delta_B v_{dc}}{2} + V_b \sin\delta \right)$$

$$i_{Bd} = -\frac{x_{dt}}{x_{d\Sigma}} \left(V_b \cos\delta + \frac{m_B \sin\delta_B v_{dc}}{2} \right) + \frac{x_{dE}}{x_{d\Sigma}} \frac{m_E \sin\delta_E v_{dc}}{2} - \frac{x_E}{x_{d\Sigma}} E_q'$$

$$i_{Bq} = -\frac{m_E \cos\delta_E v_{dc} x_{qE}}{2x_{q\Sigma}} + \frac{x_{qt}}{x_{q\Sigma}}\left(\frac{m_B \cos\delta_B v_{dc}}{2} + V_b \sin\delta\right) \quad (2.3)$$

where

$$\begin{aligned}
x_{q\Sigma} &= (x_q + x_{tE} + x_E)(x_B + x_{BV}) + x_E(x_q + x_{tE}),\\
x_{qE} &= x_q + x_{tE} \quad x_{Bq} = x_B + x_{BV} + x_q + x_{tE},\\
x_{qt} &= x_q + x_{tE} + x_E\\
x_{d\Sigma} &= (x_d' + x_{tE} + x_E)(x_B + x_{BV}) + x_E(x_d' + x_{tE}),\\
x_{dE} &= x_d' + x_{tE} \quad x_{Bd} = x_B + x_{BV} + x_d' + x_{tE},\\
x_{BB} &= x_B + x_{BV}, \quad x_{dt} = x_d' + x_{tE} + x_E
\end{aligned}$$

By use of $i_{dt} = i_{Ed} + i_{Bd}$, $i_{qt} = i_{Eq} + i_{Bq}$ and linearizing (2.2), (2.3) and the nonlinear dynamic differential equations of the power system [10], we can obtain the linearized model to be

$$\begin{bmatrix}\Delta\dot\delta\\ \Delta\dot\omega\\ \Delta\dot E_q'\\ \Delta\dot E_{fd}\end{bmatrix} = \begin{bmatrix} 0 & \omega_o & 0 & 0\\ -\frac{K_1}{M} & -\frac{D}{M} & -\frac{K_2}{M} & 0\\ -\frac{K_4}{T_{do}'} & 0 & -\frac{K_3}{T_{do}'} & \frac{1}{T_{do}'}\\ -\frac{K_A K_5}{T_A} & 0 & -\frac{K_A K_6}{T_A} & -\frac{1}{T_A}\end{bmatrix}\begin{bmatrix}\Delta\delta\\ \Delta\omega\\ \Delta E_q'\\ \Delta E_{fd}\end{bmatrix} + \begin{bmatrix}0\\ -\frac{K_{pd}}{M}\\ -\frac{K_{qd}}{T_{do}'}\\ -\frac{K_A K_{vd}}{T_A}\end{bmatrix}\Delta v_{dc} + \begin{bmatrix} 0 & 0 & 0 & 0\\ -\frac{K_{pe}}{M} & -\frac{K_{p\delta e}}{M} & -\frac{K_{pb}}{M} & -\frac{K_{p\delta b}}{M}\\ -\frac{K_{qe}}{T_{do}'} & -\frac{K_{q\delta e}}{T_{do}'} & -\frac{K_{qb}}{T_{do}'} & -\frac{K_{q\delta b}}{T_{do}'}\\ -\frac{K_A K_{ve}}{T_A} & -\frac{K_A K_{v\delta e}}{T_A} & -\frac{K_A K_{vb}}{T_A} & -\frac{K_A K_{v\delta b}}{T_A}\end{bmatrix} \cdot \begin{bmatrix}\Delta m_E\\ \Delta\delta_E\\ \Delta m_B\\ \Delta\delta_B\end{bmatrix} \quad (2.4)$$

where

$$\Delta v_{dc} = \frac{1}{K_9 + s}(K_7\Delta\delta + K_8\Delta E_q' + K_{ce}\Delta m_E + K_{c\delta e}\Delta\delta_E + K_{cb}\Delta m_B + K_{c\delta b}\Delta\delta_B) \quad (2.5)$$

If we denote

$$\Delta f_* = [\Delta v_{dc} \quad \Delta u_k]$$

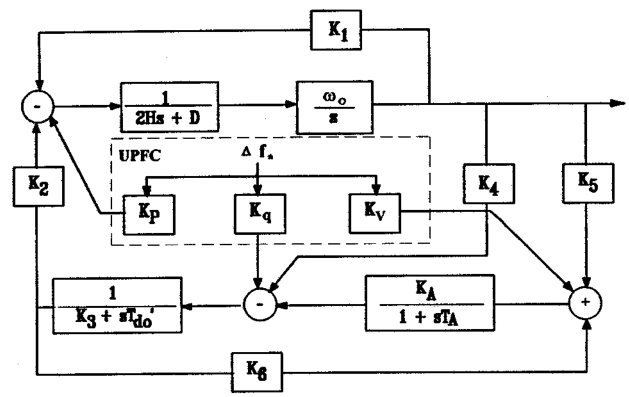

Fig. 2. The linearized Phillips–Heffron model.

$$K_P = \begin{bmatrix}\frac{K_{pd}}{M}\\ \frac{K_{pu_k}}{M}\end{bmatrix}, \quad K_q = \begin{bmatrix}\frac{K_{qd}}{T_{d0}'}\\ \frac{K_{qu_k}}{T_{d0}'}\end{bmatrix}, \quad K_V = \begin{bmatrix}\frac{K_A K_{vd}}{T_A T_{d0}'}\\ \frac{K_A K_{vu_k}}{T_A T_{d0}'}\end{bmatrix} \quad (2.6)$$

the linearized model of (2.4) can be shown by Fig. 2, where u_k is the input control signal to the UPFC which could be m_E, m_B, δ_E or δ_B. From Fig. 2 we can see that the linearized model is of the exactly same form of the unified Phillips–Heffron model for SVC, TCSC and TCPAR [10].

III. Multi-Machine Power Systems

Without loss of generality, we assume that in an n-machine power system, a UPFC is installed between nodes 1 and 2 as shown by Fig. 3. Thus we have

$$\begin{aligned}
\overline{Y}_{11}'\overline{V}_1 + \overline{I}_{1E} + \overline{\mathbf{Y}}_{\mathbf{13}}\overline{\mathbf{V}}_{\mathbf{g}} &= 0\\
\overline{Y}_{22}'\overline{V}_2 - \overline{I}_{E2} + \overline{\mathbf{Y}}_{\mathbf{23}}\overline{\mathbf{V}}_{\mathbf{g}} &= 0\\
\overline{\mathbf{Y}}_{\mathbf{31}}\overline{V}_1 + \overline{\mathbf{Y}}_{\mathbf{32}}\overline{V}_2 + \overline{\mathbf{Y}}_{\mathbf{33}}\overline{\mathbf{V}}_{\mathbf{g}} &= \overline{\mathbf{I}}_{\mathbf{g}}
\end{aligned} \quad (3.1)$$

where $\overline{Y}_{11}'$ and $\overline{Y}_{22}'$ are self admittance at node 1 and 2 with $x_{12} = x_{1E} + x_{E2}$ excluded and

$$\overline{\mathbf{I}}_{\mathbf{g}} = [\overline{I}_{g1} \quad \overline{I}_{g2} \quad \cdots \quad \overline{I}_{gn}]^T,$$
$$\overline{\mathbf{V}}_{\mathbf{g}} = [\overline{V}_{g1} \quad \overline{V}_{g2} \quad \cdots \quad \overline{V}_{gn}]^T$$

From Fig. 3 we can have

$$\begin{aligned}
\overline{V}_1 &= jx_{1E}\overline{I}_{1E} + \overline{V}_{Et}\\
\overline{V}_{Et} &= jx_{E2}\overline{I}_{E2} + \overline{V}_{Bt} + \overline{V}_2, \; \overline{I}_E = \overline{I}_{1E} - \overline{I}_{E2}
\end{aligned} \quad (3.2)$$

From (3.2) and (2.1) we can obtain

$$\begin{bmatrix}\overline{I}_{1E}\\ \overline{I}_{E2}\end{bmatrix} = \frac{1}{x_\Sigma}\begin{bmatrix}-j(x_E + x_{E2} + x_B) & jx_E\\ -jx_E & j(x_{1E} + x_E)\end{bmatrix}\begin{bmatrix}\overline{V}_1\\ \overline{V}_2\end{bmatrix} + \frac{1}{x_\Sigma}\begin{bmatrix}j(x_{E2} + x_B) & jx_E\\ -jx_E & j(x_{1E} + x_E)\end{bmatrix}\begin{bmatrix}\overline{V}_E\\ \overline{V}_B\end{bmatrix} \quad (3.3)$$

where $x_\Sigma = (x_{1E} + x_E)(x_E + x_{E2} + x_B) - x_E^2$. Then by substituting (3.3) into (3.1) we can have

$$\overline{\mathbf{I}}_{\mathbf{g}} = \overline{\mathbf{C}}\overline{\mathbf{V}}_{\mathbf{g}} + \overline{\mathbf{F}}_{\mathbf{E}}\overline{V}_E + \overline{\mathbf{F}}_{\mathbf{B}}\overline{V}_B \quad (3.4)$$

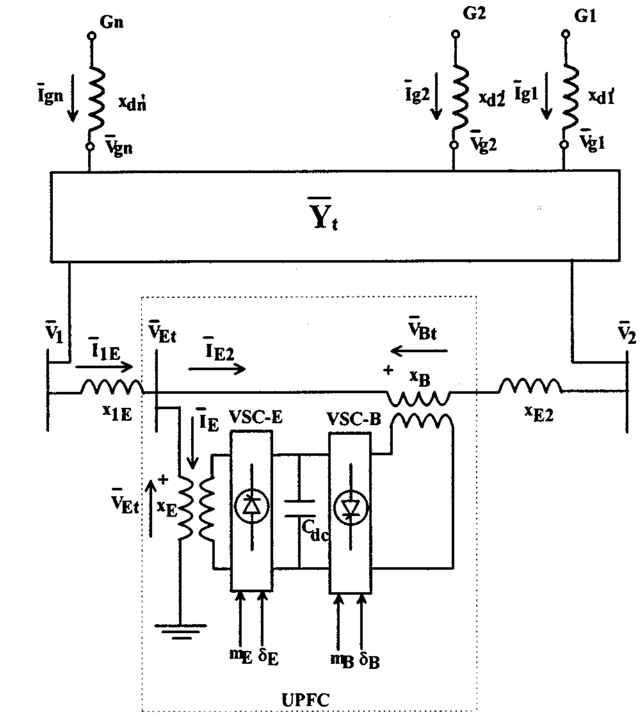

Fig. 3. An n-machine power system installed with a UPFC.

where

$$\overline{\mathbf{C}} = \overline{\mathbf{Y}}_{\mathbf{33}} - [\,\overline{\mathbf{Y}}_{\mathbf{31}} \quad \overline{\mathbf{Y}}_{\mathbf{31}}\,]\,\overline{\mathbf{Y}}_{\mathbf{t}}'^{-1} \begin{bmatrix} \overline{\mathbf{Y}}_{\mathbf{13}} \\ \overline{\mathbf{Y}}_{\mathbf{23}} \end{bmatrix}$$

$$\overline{\mathbf{F}}_{\mathbf{E}} = -[\,\overline{\mathbf{Y}}_{\mathbf{31}} \quad \overline{\mathbf{Y}}_{\mathbf{31}}\,]\,\overline{\mathbf{Y}}_{\mathbf{t}}'^{-1} \begin{bmatrix} \dfrac{j(x_{E2}+x_B)}{x_\Sigma} \\ \dfrac{jx_{E1}}{x_\Sigma} \end{bmatrix}$$

$$\overline{\mathbf{F}}_{\mathbf{B}} = -[\,\overline{\mathbf{Y}}_{\mathbf{31}} \quad \overline{\mathbf{Y}}_{\mathbf{31}}\,]\,\overline{\mathbf{Y}}_{\mathbf{t}}'^{-1} \begin{bmatrix} \dfrac{jx_E}{x_\Sigma} \\ \dfrac{-j(x_{1E}+x_E)}{x_\Sigma} \end{bmatrix}$$

$$\overline{\mathbf{Y}}_{\mathbf{t}}' = \begin{bmatrix} \overline{Y}_{11}' - \dfrac{j(x_E+x_{E2}+x_B)}{x_\Sigma} & \dfrac{jx_E}{x_\Sigma} \\ \dfrac{jx_E}{x_\Sigma} & \overline{Y}_{22}' - \dfrac{j(x_{1E}+x_E)}{x_\Sigma} \end{bmatrix}$$

For the n-machine power system, the terminal voltage of the generators can also be expressed in the common coordinates as [12] $\overline{\mathbf{V}}_{\mathbf{g}} = \overline{\mathbf{E}}_{\mathbf{q}}' - j\mathbf{x}_{\mathbf{d}}'\overline{\mathbf{I}}_{\mathbf{g}} - j(\mathbf{x}_{\mathbf{q}} - \mathbf{x}_{\mathbf{d}}')\overline{\mathbf{I}}_{\mathbf{q}}$, from which and (3.4) we can obtain

$$\mathbf{I}_{\mathbf{g}} = \overline{\mathbf{C}}_{\mathrm{d}}[\overline{\mathbf{E}}_{\mathbf{q}}' - j(\mathbf{x}_{\mathbf{q}} - \mathbf{x}_{\mathbf{d}}')\overline{\mathbf{I}}_{\mathbf{q}} + \overline{\mathbf{C}}_{\mathbf{E}}\overline{V}_E + \overline{\mathbf{C}}_{\mathbf{B}}\overline{V}_B] \qquad (3.5)$$

where $\overline{\mathbf{C}}_{\mathbf{d}} = (\overline{\mathbf{C}}^{-1} + j\mathbf{x}_{\mathbf{d}}')^{-1}$, $\overline{\mathbf{C}}_{\mathbf{E}} = \overline{\mathbf{C}}^{-1}\overline{\mathbf{F}}_{\mathbf{E}}$, $\overline{\mathbf{C}}_{\mathbf{B}} = \overline{\mathbf{C}}^{-1}\overline{\mathbf{F}}_{\mathbf{B}}$. In $d_i - q_i$ coordinates, the linearized form of (3.5) is

$$\begin{aligned} \Delta\mathbf{I}_{\mathbf{q}} = {} & \mathbf{Y}_{\mathbf{q}}\Delta\delta + \mathbf{F}_{\mathbf{q}}\Delta\mathbf{E}_{\mathbf{q}}' + \mathbf{G}_{\mathbf{q}}\Delta v_{dc} + \mathbf{H}_{\mathbf{Eq}}\Delta m_E \\ & + \mathbf{H}_{\mathbf{Bq}}\Delta m_B + \mathbf{R}_{\mathbf{Eq}}\Delta\delta_E + \mathbf{R}_{\mathbf{Bq}}\Delta\delta_B \qquad (3.6a) \end{aligned}$$

$$\begin{aligned} \Delta\mathbf{I}_{\mathbf{d}} = {} & \mathbf{Y}_{\mathbf{d}}\Delta\delta + \mathbf{F}_{\mathbf{d}}\Delta\mathbf{E}_{\mathbf{q}}' + \mathbf{G}_{\mathbf{d}}\Delta v_{dc} + \mathbf{H}_{\mathbf{Ed}}\Delta m_E \\ & + \mathbf{H}_{\mathbf{Bd}}\Delta m_B + \mathbf{R}_{\mathbf{Ed}}\Delta\delta_E + \mathbf{R}_{\mathbf{Bd}}\Delta\delta_B \qquad (3.6b) \end{aligned}$$

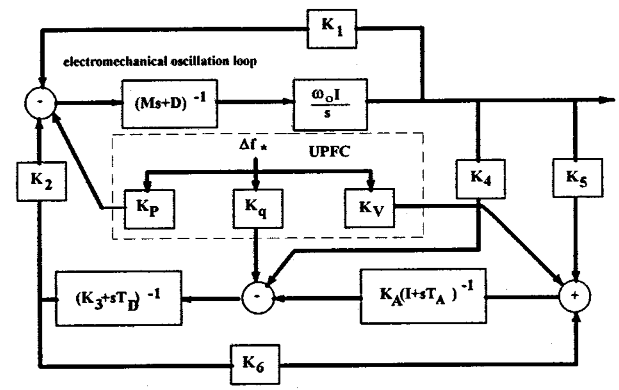

Fig. 4. The linearized Phillips–Heffron model.

Substituting (3.6) into the linearized dynamic equations of the n-machine power system [11] we can obtain (3.7) at the bottom of the next page. If we denote

$$\Delta\mathbf{f}_* = [\,\Delta v_{dc} \quad \Delta u_k\,], \quad \mathbf{K}_{\mathbf{P}} = \begin{bmatrix} \mathbf{M}^{-1}\mathbf{K}_{\mathbf{pd}} \\ \mathbf{M}^{-1}\mathbf{K}_{\mathbf{pu_k}} \end{bmatrix},$$

$$\mathbf{K}_{\mathbf{q}} = \begin{bmatrix} \mathbf{T}_{\mathbf{d0}}'^{-1}\mathbf{K}_{\mathbf{qd}} \\ \mathbf{T}_{\mathbf{d0}}'^{-1}\mathbf{K}_{\mathbf{qu_k}} \end{bmatrix}, \quad \mathbf{K}_{\mathbf{V}} = \begin{bmatrix} \mathbf{T}_{\mathbf{A}}^{-1}\mathbf{K}_{\mathbf{A}}\mathbf{K}_{\mathbf{vd}} \\ \mathbf{T}_{\mathbf{A}}^{-1}\mathbf{K}_{\mathbf{A}}\mathbf{K}_{\mathbf{vu_k}} \end{bmatrix}$$

the linearized model of (3.7) can be shown by Fig. 4, where u_k could be m_E, m_B, δ_E or δ_B. Obviously, the model is of the exactly same form as that of the unified model for SVC, TCSC and TCPAR presented in [11].

IV. Effect of UPFC DC Voltage Regulator on Power System Oscillation Stability

For the continuous and effective operation of a UPFC, the DC voltage across the UPFC link capacitor must be kept constant, which can be achieved by installing a DC voltage regulator $u_k = T_{\mathrm{DC}}(s)(v_{dcref} - v_{dc})$ in the UPFC [2], [3]. The DC voltage regulator functions by controlling the exchange of active power between the UPFC and the power system. Hence its influence upon power system oscillation damping should be expected and can be investigated based on the Phillips–Heffron model developed above.

For example, if it is assumed that the active power input to the UPFC installed in the single-machine infinite-bus power system of Fig. 1 is $P_{\mathrm{UPFC}} = v_{dc}I_{dc}$. The power balance equation of the power system should be $P_m - P_e = P_{acc} + P_{\mathrm{UPFC}}$, where P_m(constant) is the mechanical power input to the generator, P_e the electric power output from the generator and P_{acc} the accelerating power to the rotor movement of the generator. At steady-state operation, $P_{m0} - P_{e0} = 0$ since $P_{acc0} = 0$ and $P_{\mathrm{UPFC0}} = v_{dc0}I_{dc0} = 0\,(I_{dc0} = 0)$. During the dynamic process, the power balance is achieved to ensure $\Delta P_e + \Delta P_{acc} + \Delta P_{\mathrm{UPFC}} = 0$. Thus ΔP_{UPFC} varies in opposition to that of ΔP_e as ΔP_{acc} does so that the active power is kept in balance. Therefore, ΔP_{UPFC} is opposite to ΔP_e in phase and thus leads $\Delta\omega$ by 90 degrees. Since $C_{dc}\dot{v}_{dc} = I_{dc}$ [3], we can have $\Delta P_{\mathrm{UPFC}} = v_{dc0}\Delta I_{dc} + I_{dc0}\Delta v_{dc} = v_{dc0}\Delta I_{dc} = sCV_{dc0}\Delta v_{\mathrm{DC}}$. So Δv_{dc} lags ΔP_{UPFC} by 90 degrees in phase and hence in the same phase with $\Delta\omega$, which can be expressed as $\Delta v_{dc} = K_{\mathrm{DC}\omega}\Delta\omega$.

Therefore, from the unified model of the power system installed with the UPFC of Fig. 2, we can obtain the "direct electric torque" [10] contribution from the UPFC DC voltage regulator to the electromechanical oscillation loop of the generator to be $\Delta T_{EDC} = -K_{Pu_k}T_{\mathrm{DC}}(j\omega_s)\Delta v_{dc} = -K_{Pu_k}T_{\mathrm{DC}}(j\omega_s)K_{\mathrm{DC}\omega}\Delta\omega$. Hence, if the DC voltage regulator is a PI controller and $K_{Pu_k} > 0$, the proportional control of the DC voltage regulator will provide the power system with negative damping torque. Whilst the integral control of the DC voltage regulator contributes no damping to system oscillations.

Parameters of an example single-machine infinite-bus power system to be installed with a UPFC are given in the Appendix. It is used to confirm the simple analysis above and demonstrate the negative effect of the UPFC DC voltage regulator on power system oscillation stability. The UPFC is equipped with power flow, voltage control function and a DC voltage regulator,

$$(\mathrm{P}): \quad u_k = m_B = K_{Pf}(P_{eref} - P_e),$$
power flow controller

$$(\mathrm{AC}): \quad u_k = m_E = K_{VEt}(v_{Etref} - v_{Et}),$$
AC voltage regulator

$$(\mathrm{DC}): \quad u_k = \delta_E = K_{\mathrm{DC}}(v_{dcref} - v_{dc}),$$
DC voltage regulator

From the Phillips–Heffron model of the power system we obtain $K_{P\delta e} = 1.1503 > 0$, which indicates that the UPFC DC voltage regulator damages system oscillation stability. Table I presents the results of Damping Torque (DT) and oscillation mode computation from system Phillips–Heffron model, from which we can see that

1) UPFC DC voltage regulator supplies negative damping torque and reduces the damping of system oscillation mode, as indicated by the simple analysis;
2) UPFC power flow and voltage controller have little influence on system oscillation damping.

TABLE I
DAMPING TORQUE (DT) CONTRIBUTION AND INFLUENCE OF THE UPFC CONTROL ON SYSTEM OSCILLATION MODE

study case	DT	oscillation mode	damping ratio (ζ) and frequency (f)
no UPFC	0.0	$-0.1834 \pm j4.6694$	$\zeta = 0.04, f = 0.74$
with (P)	0.0	$-0.1721 \pm j4.4505$	$\zeta = 0.04, f = 0.71$
with (AC)	0.0	$-0.1850 \pm j4.3361$	$\zeta = 0.04, f = 0.69$
with (DC)	-3.1	$-0.0550 \pm j4.4588$	$\zeta = 0.01, f = 0.71$

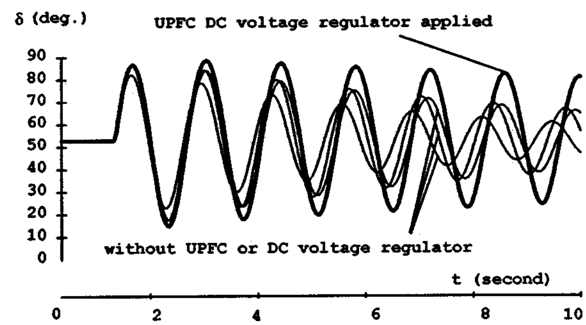

Fig. 5. Non-linear simulation to test the effect of UPFC control on system oscillation damping.

Fig. 5 gives the confirmation from the nonlinear simulation where a three-phase to-earth short circuit occurs on the transmission line between the UPFC bus and the infinite bus at 1.0 second and is cleared after 100 ms. Fig. 6 shows the variation of various signals which confirms that Δv_{dc} varies in the same

$$\dot{\mathbf{X}} = \mathbf{AX} + \mathbf{B}\Delta\mathbf{u} \tag{3.7}$$

where

$$\mathbf{A} = \begin{bmatrix} 0 & \omega_o\mathbf{I} & 0 & 0 & 0 \\ -\mathbf{M}^{-1}\mathbf{K_1} & -\mathbf{M}^{-1}\mathbf{D} & -\mathbf{M}^{-1}\mathbf{K_2} & 0 & -\mathbf{M}^{-1}\mathbf{K_{pd}} \\ -\mathbf{T'^{-1}_{do}}\mathbf{K_4} & 0 & -\mathbf{T'^{-1}_{do}}\mathbf{K_3} & \mathbf{T'^{-1}_{do}} & -\mathbf{T'^{-1}_{do}}\mathbf{K_{qd}} \\ -\mathbf{T_A^{-1}}\mathbf{K_A}\mathbf{K_5} & 0 & -\mathbf{T_A^{-1}}\mathbf{K_A}\mathbf{K_6} & -\mathbf{T_A^{-1}} & -\mathbf{T_A^{-1}}\mathbf{K_A}\mathbf{K_{vd}} \\ \mathbf{K_7} & 0 & \mathbf{K_8} & 0 & -K_9 \end{bmatrix}$$

$$\mathbf{B} = \begin{bmatrix} 0 & 0 & 0 & 0 \\ -\mathbf{M}^{-1}\mathbf{K_{pe}} & -\mathbf{M}^{-1}\mathbf{K_{pde}} & -\mathbf{M}^{-1}\mathbf{K_{pb}} & -\mathbf{M}^{-1}\mathbf{K_{pdb}} \\ -\mathbf{T'^{-1}_{do}}\mathbf{K_{qe}} & -\mathbf{T'^{-1}_{do}}\mathbf{K_{qde}} & -\mathbf{T'^{-1}_{do}}\mathbf{K_{qb}} & -\mathbf{T'^{-1}_{do}}\mathbf{K_{qdb}} \\ -\mathbf{T_A^{-1}}\mathbf{K_A}\mathbf{K_{ve}} & -\mathbf{T_A^{-1}}\mathbf{K_A}\mathbf{K_{vde}} & -\mathbf{T_A^{-1}}\mathbf{K_A}\mathbf{K_{vb}} & -\mathbf{T_A^{-1}}\mathbf{K_A}\mathbf{K_{vdb}} \\ K_{ce} & K_{c\delta e} & K_{cb} & K_{c\delta b} \end{bmatrix}$$

$$\mathbf{X} = [\Delta\delta^T \quad \Delta\omega^T \quad \Delta\mathbf{E'_q} \quad \Delta\mathbf{E_{FD}} \quad \Delta v_{dc}]^T$$

$$\Delta\mathbf{u} = [\Delta m_E \quad \Delta\delta_E \quad \Delta m_B \quad \Delta\delta_B]^T$$

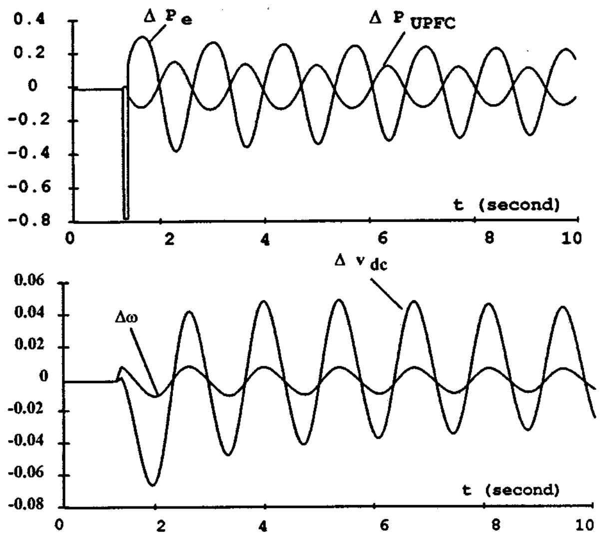

Fig. 6. Non-linear simulation with UPFC installed.

phase with $\Delta\omega$ and ΔP_{UPFC} is opposite to ΔP_e as indicated by the simple analysis.

V. Selection of UPFC Input Control Signals for Applying Damping Control

To introduce a damping function into the UPFC, the output control signal from the damping controller can be selected among m_E, m_B, δ_E and δ_B so that a most effective damping control can be achieved (to obtain the satisfactory damping control at minimum control cost, i.e., lowest gain value of the damping controller). Based on the Phillips–Heffron model, the selection can be made as follows.

The state equation of the power system of (2.4) and (3.7) can be arranged to be

$$\begin{bmatrix} \Delta\dot{\delta}_j \\ \Delta\dot{\omega}_j \\ \dot{\mathbf{x}} \end{bmatrix} = \begin{bmatrix} 0 & \omega_0 & \mathbf{0} \\ -k_j & -d_j & \mathbf{A_{23}} \\ \mathbf{A_{31}} & \mathbf{A_{32}} & \mathbf{A_{33}} \end{bmatrix} \begin{bmatrix} \Delta\delta_j \\ \Delta\omega_j \\ \mathbf{x} \end{bmatrix} + \begin{bmatrix} 0 \\ B_2 \\ \mathbf{B_3} \end{bmatrix} \Delta u_k$$

Then it can be proved that $b_i(\lambda_i) = K_{bi}(\lambda_i)w_{i2}$ [13], where $K_{bi}(\lambda_i) = B_2 + \mathbf{A_{23}}(\lambda_i\mathbf{I} - \mathbf{A_{33}})^{-1}\mathbf{B_3}$, $b_i(\lambda_i)$ is the controllability index of the UPFC damping controller on the oscillation mode λ_i of interest and w_{i2} is the ith element of the left eigenvector of system state matrix associated with λ_i. From (2.4) and (3.7) it can be seen that for different input control signals of the UPFC, only $K_{bi}(\lambda_i)$ changes. Therefore, to the oscillation mode of interest λ_i, m_E, m_B, δ_E and δ_B have same value of w_{i2} and modal observability index $c_i(\lambda_i)$. Therefore, $|K_{bi}(\lambda_i)|$can be used for the selection of the most effective input control signal among m_E, m_B, δ_E and δ_B. In the following, this application based on the Phillips–Heffron model of the power system installed with the UPFC will be demonstrated by an example three-machine power system as shown by Fig. 7, the parameters of which are given in Appendix. A low-frequency oscillation of around 0.6 Hz has been observed in the power system. The responsible oscillation mode is $\lambda_i = -0.0877 \pm j3.6284$. A UPFC is to be installed at the middle point of the transmission line between node 3 and 4. It is decided that a damping controller will be designed as one of the secondary functions of the UPFC to damp the low-frequency oscillation. The locally available active line power delivered along the transmission line will be adopted as the feedback signal of the damping controller.

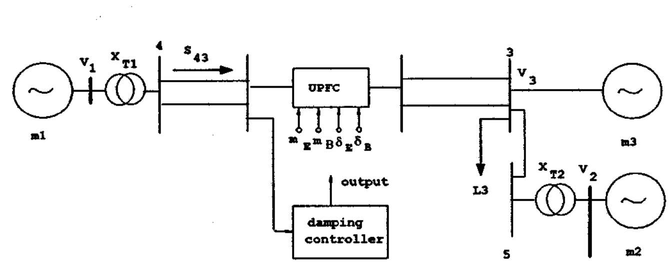

Fig. 7. The example power system.

TABLE II
CALCULATION RESULTS BASED ON THE PHILLIPS-HEFFRON MODEL

u_k	$\lvert K_{bi}(\lambda_i)\rvert_{u_k}$	λ_i	ζ and f
m_E	0.2976	$\lambda = -0.30 \pm j2.86$	$\zeta = 0.1, f = 0.45$
m_B	0.1493	$\lambda = -0.51 \pm j4.90$	$\zeta = 0.1, f = 0.78$
δ_E	0.0683	$\lambda = -0.36 \pm j3.17$	$\zeta = 0.1, f = 0.50$
δ_B	0.0	$\lambda = -0.09 \pm j3.63$	$\zeta = 0, f = 0.58$

To select the input control signal of the UPFC among m_E, m_B, δ_E and δ_B, the index $|K_{bi}(\lambda_i)|_{u_k}$ for u_k to be m_E, m_B, δ_E and δ_B is calculated respectively from system Phillips–Heffron model. The results are given in Table II. From Table II it can be seen that the calculation of $|K_{bi}(\lambda_i)|_{u_k}$ predicts that the most effective signal is m_E for the design of the damping controller.

To confirm the prediction, a pure-gain damping controller is designed and installed. To achieve an improvement of the damping ratio of the oscillation mode to around 0.1, the gain value of the damping controller, K, has to be set to be 1) $K = 4.0$ when $u_k = m_E$; 2) $K = 6.0$ when $u_k = m_B$; 3) $K = 10.0$ when $u_k = \delta_E$; 4) The oscillation mode is uncontrollable when $u_k = \delta_B$. The assignment of the oscillation mode by the damping controller is shown in the third column in Table II. Fig. 8 presents the nonlinear simulation when the pure-gain damping controller is applied. The oscillation is triggered by a three-phase short circuit occurring on the transmission line between node 3 and 5 in the example power system at 1.0 second of the simulation and is cleared after 100 ms.

Obviously, the application of the pure-gain damping control justifies that $u_k = m_E$ is the best selection for the design of the UPFC damping controller since the minimum control cost (the lowest gain) is needed to provide the required damping. This confirms the prediction by $|K_{bi}(\lambda_i)|_{u_k}$ calculated from the linearized model of the power system. Fig. 8 also shows the negative damping effect of UPFC DC voltage regulator.

VI. Conclusions

The major contributions of this paper are

1) Establishment of the linearized Phillips–Heffron model of single-machine and multi-machine power systems

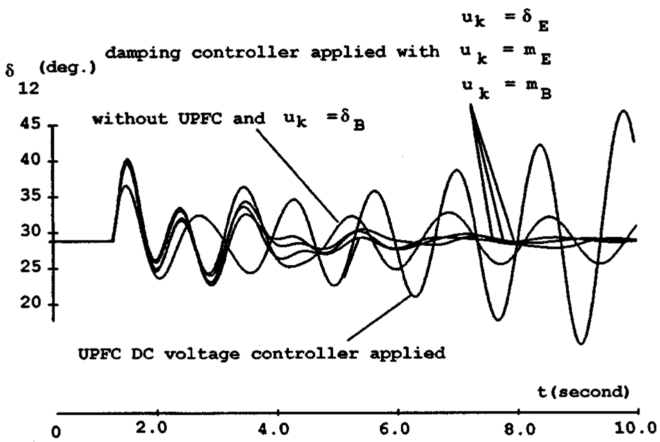

Fig. 8. Non-linear simulation of the three-machine example power system installed with a UPFC.

installed with a UPFC, which adds the UPFC into the category of FACTS controllers for their unified model [10], [11].

2) The applications of the Phillips–Heffron model are demonstrated by 1) studying the effect of UPFC DC voltage regulator on power system oscillation stability; 2) selecting the most effective damping control signals for the design of the UPFC damping controller.

APPENDIX

Example single-machine infinite-bus power system:

$$\begin{aligned} H &= 4.0 \text{ s.}, \quad D = 0.0, \quad T'_{d0} = 5.044 \text{ s.}, \quad x_d = 1.0, \\ x_q &= 0.6, \quad x'_d = 0.3, \quad x_T = 0.03, \quad x_{tE} = x_{EB} = 0.3, \\ K_A &= 10.0, \quad T_A = 0.01 \text{ s.}, \quad v_{dc0} = 10 \text{ kv}, \\ K_{Pf} &= 10.0, \quad K_{VEt} = 10.0, \quad K_{\mathrm{DC}} = 2.0 \text{ p.u.}, \\ P_{e0} &= 1.0, \quad V_{B0} = V_{t0} = 1.0, \end{aligned}$$

$$T_{\mathrm{DC}} \text{ (converter time constant)} = 0.01 \text{ s.}$$

Example three-machine power system:

$$\begin{aligned} H_1 &= H_2 = 20.09 \text{ s.}, \quad H_3 = 11.8 \text{ s.}, \\ D_1 &= D_2 = D_3 = 0.0, \quad T'_{d01} = T'_{d02} = 7.5 \text{ s.}, \\ T'_{d03} &= 4.7 \text{ s.}, \quad x_{d1} = x_{d2} = 0.19, \quad x_{d3} = 0.41 \\ x_{q_1} &= x_{q_2} = 0.163, \quad x_{q_3} = 0.33, \\ x'_{d1} &= x'_{d2} = 0.0765, \\ x'_{d3} &= 0.173 \quad K_{A1} = K_{A3} = 20.0, \\ K_{A2} &= 100, \quad T_{A1} = T_{A3} = 0.05 \text{ s.}, \\ T_{A2} &= 0.01 \text{ s.} \quad \overline{Z}_{13} = j0.6 \text{ (double lines)}, \\ \overline{Z}_{23} &= j0.1 \quad \overline{Z}_{T1} = \overline{Z}_{T2} = j0.03 \quad \overline{V}_{1t} = 1.0\angle 14^\circ, \\ \overline{V}_{2t} &= 1.0\angle 5^\circ, \quad \overline{V}_{3t} = 1.0\angle 0^\circ \quad L_3 = 1.07 + j1.0 \\ K_{\mathrm{DC}} &= 5.0, \quad T_{\mathrm{DC}} = 0.01 \text{ s.} \end{aligned}$$

REFERENCES

[1] L. Gyugyi, “Unified power-flow control: Concept for flexible AC transmission systems,” *IEE Proc.C*, no. 4, 1992.

[2] L. Gyugyi, T. R. Rietman, A. Edris, C. D. Schauder, D. R. Torgerson, and S. L. Williams, “The unified power flow controller: A new approach to power transmission control,” *IEEE Trans. on PWRS*, no. 2, 1995.

[3] A. Nabavi-Niaki and M. R. Iravani, “Steady-state and dynamic models of unified power flow controller (UPFC) for power system studies,” *IEEE Trans. on PWRS*, no. 4, 1996.

[4] A. Arabi and P. Kundur, “A versatile FACTS device model for power flow and stability simulation,” *IEEE Trans. on PWRS*, no. 4, 1996.

[5] E. V. Larsen, J. J. Sanchez-Gasca, and J. H. Chow, “Concept for design of FACTS controllers to damp power swings,” *IEEE Trans. on PWRS*, no. 2, 1995.

[6] M. Noroozian and G. Andersson, “Damping of power system oscillations by use of controllable components,” *IEEE Trans. on PWRD*, no. 4, 1994.

[7] S. Nyati, C. A. Wenger, R. W. Delmerico, D. H. Baker, R. J. Piwko, and A. Edris, “Effectiveness of thyristor controlled series capacitor in enhancing power system dynamics: An analogue simulator study,” *IEEE on PWRD*, no. 2, 1994.

[8] F. P. deMello and C. Concordia, “Concept of synchronous machine stability as affected by excitation control,” *IEEE Trans. on PAS*, no. 2, 1969.

[9] W. G. Heffron and R. A. Phillips, “Effect of a modern amplidyne voltage regulator on under excited operation of large turbine generator,” *AIEE Trans.*, 1952.

[10] H. F. Wang and F. J. Swift, “An unified model for the analysis of FACTS devices in damping power system oscillations Part I: Single-machine infinite-bus power systems,” *IEEE Trans. on PWRD*, no. 2, 1997.

[11] H. F. Wang, F. J. Swift, and M. Li, “An unified model for the analysis of FACTS devices in damping power system oscillations Part II: Multi-machine power systems,” *IEEE Trans. on PWRD*, no. 4, 1998.

[12] Y. N. Yu, *Electric Power System Dynamics*: Academic Press, 1983.

[13] H. F. Wang, “Selection of robust installing locations and feedback signals of FACTS-based stabilizers in multi-machine power systems,” *IEEE Trans. on PWRS*, no. 2, 1999.

HaiFeng Wang is a Lecturer in University of Bath, U.K. His research interests are power system analysis and control. He is a Chartered Engineer.